ARCHIVES
of
FOUNDRY ENGINEERING
DOI: 10.2478/afe-2013-0001
Published quarterly as the organ of the Foundry Commission of the Polish Academy of Sciences
ISSN (2299-2944)
Volume 13
Issue 1/2013
5 – 8

Influence of Vibrations During Crystallization on Mechanical Properties and Porosity of EN AC-AlSi17 Alloy

T. Ciućka
Department of Technology of Machinery and Automation, Faculty of Chipless Forming Technology,
University of Bielsko-Biała, Willowa 2, 43- 300 Bielsko - Biała, Poland
Corresponding author. E-mail address: tciucka@ath.bielsko.pl

Received 29.06. 2012; accepted in revised form 04.09.2012

Abstract

Today's industry aims at such situation, where number of defective products, so called defects shall approach to zero. Therefore, one introduces a various changes in technology of production, introduces improvements which would help in accomplishment of this objective. Another important factor is introduction of different type of testing, which shall help in assessment which factor has significant effect on quantity of rejects, and which one could be neglected. Existence of casting rejects is unavoidable; therefore a new ideas, technologies and innovations are necessary in the entire widely understood foundry branch, in order to minimize such adverse effect. Performance of tests aimed at unequivocal determination of an effect of vibrations during crystallization on mechanical properties and porosity of the EN AC-AlSi17 alloy was the objective of the present work. To do this, there were produced 36 castings from EN AC-AlSi17 alloy. All the castings underwent machining operations. Half of the casting was destined to strength tests, the other half served to determination of an effect of vibrations on porosity of the alloy. The specimens were divided into 12 groups, depending on amplitude of vibrations and tilt angle of metal mould during pouring operation.

Keywords: Fundamentals of foundry processes, Crystallization, Structural constituent, Porosity, ATD

1. Introduction

For the testing one prepared 36 specimens from EN AC-AlSi17 alloy, the specimens were poured in foundry laboratory of University in Bielsko – Biala. As the first sequence there were cast 18 specimens destined to determination an effect of vibrations during crystallization on phenomenon of porosity. Subsequently, one poured next 18 specimens destined to the testing aimed at determination of an effect of vibrations during crystallization on mechanical properties.

The tests were performed with not modified alloy, refined in temperature of 720^{0}C. In the process of refinement one used Rafa1 rafinator (hexachloroethan) in quantity 0,05%wt. of mass of the metallic charge.

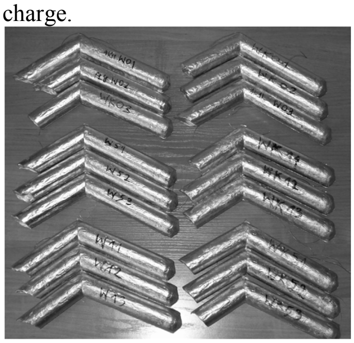

Fig. 1. Batch of poured specimens

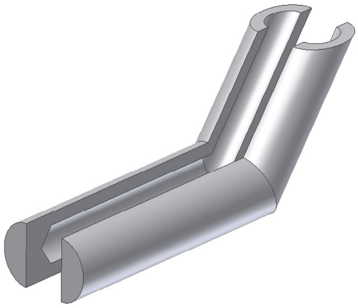

Fig. 2. Metal mould used to pouring of the tested specimens

The metal mould had a possibility of installation of a thermocouple, which served to permanent registration, in real time, of temperature of solidifying specimen. With use of measuring station of the ATD method one registered runs of crystallization for individual specimens. Results of the registration were presented in graphic form on crystallization diagrams from the ATD method [7, 8, 9,10]. The tests were performed in fixed conditions. One poured specimens of the investigated alloy in the following conditions: without vibrations, with 50% amplitude of the vibrations (0,4 mm), with 100% amplitude of the vibrations (0,8 mm), frequency of vibration of 50Hz, temperature of metal mould of 250^0C, temperature of the alloy of 760^0C. Half of the specimens (18) were poured in horizontal position, whereas the second half of the specimens were poured in metal mould tilted with 20^0 (Fig. 3). Three pieces of specimens for each series were produced. [12, 13]

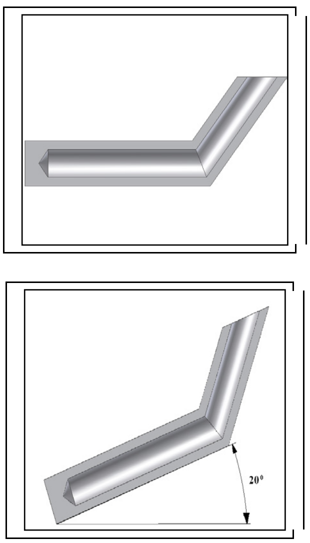

Fig. 3. Positioning of the metal mould during pouring

2. Methodology of the investigations

The paper presents test results of an effect of metal mould vibrations on crystallization of the investigated EN AC-AlSi17 alloy. The Table 1 below presents method of marking of the specimens. In the Fig4. is shown an exemplary result of registration with use of the ATD method of the given specimen.

Aluminum industry has a great contribution to world-wide economy. Nowadays, aluminum is the second (after steel) the most popular and the most often used metal in the world [1]. For a few last decades its production has grown nearly ten times and is still growing. The aluminum owes its popularity to properties like corrosion resistance or thermal and electric conductivity. However, ratio of the strength to mass is the main property. Except advantages, the aluminum also features a disadvantage like the price is. Alloys of aluminum with silicon (so called silumins), which are characterized by good mechanical properties, find broad applications in electro-engineering, automotive, aircraft, precise, household equipment industry, and in many other industrial branches [2, 3, 4]. Contemporary tendencies striving after minimization of mass of structures should increase field of the application. [14]

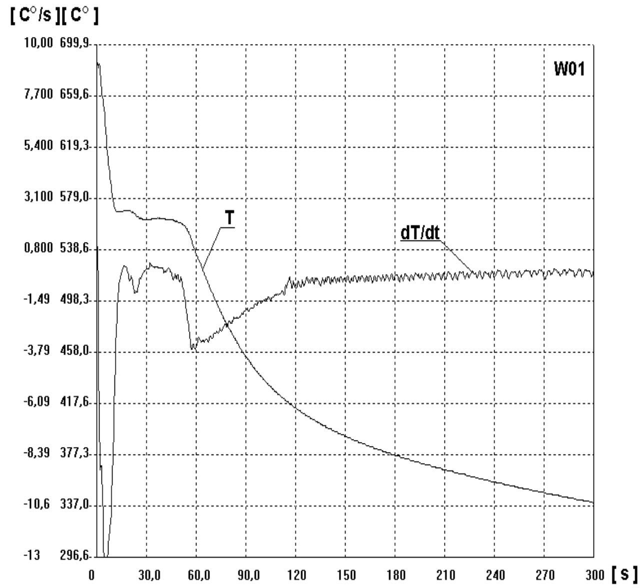

Fig. 4. The ATD diagram of the 1113 specimen

Test bed to investigation of porosity of the alloy consisted of the NEOPHOT 32 metallographic microscope equipped with high resolution camera connected to computerized system of image analysis. Next, with use of the *MULTISCAN* program there were performed photos of the investigated specimens (Fig. 5). Successive stage consisted on generation, with use of the image analyzer system, an image of specimens' photos showing areas of porosity and contraction cavities only, on base of which the software could calculate surface area of the porosities and contraction cavities. [15]

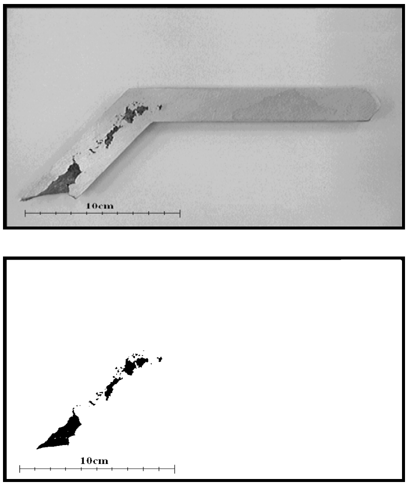

Fig. 5. Exemplary view of 01specimen together with generated by the image analyzer system surface of porosity

Table 1.
Marking of the specimens

Marking of the specimen	Vibrations[%]	Tilt angle of metal mould [deg]	Number of specimen in the series
1101	0	0	1
1102	0	0	2
1103	0	0	3
1151	50	0	1
1152	50	0	2
1153	50	0	3
1111	100	0	1
1112	100	0	2
1113	100	0	3
K1101	0	20	1
K1102	0	20	2
K1103	0	20	3
K1151	50	20	1
K1152	50	20	2
K1153	50	20	3
K1111	100	20	1
K1112	100	20	2
K1113	100	20	3

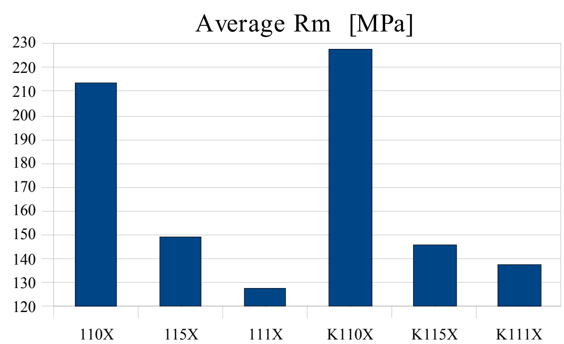

Fig. 6. Results of strength tests of the EN AC-AlSi17 alloy

Results of the porosity tests are summarized in the Table 2.

Table 2.
List of superficial porosity test results

Marking of the specimen	Porosity surface area [cm^2]	Percentage share [%]	Porosity average surface area [cm^2]
1101	1,34	0,21	
1102	1,16	0,19	1,28
1103	0,97	0,15	
1151	2,07	0,33	
1152	0,93	0,16	1,42
1153	1,28	0,20	
1111	1,12	0,18	
1112	0,83	0,13	0,95
1113	0,91	0,14	
K1101	0,72	0,12	
K1102	0,75	0,12	0,77
K1103	0,83	0,13	
K1151	1,34	0,21	
K1152	0,97	0,15	1,18
K1153	1,23	0,2	
K1111	0,84	0,13	
K1112	0,83	0,13	0,86
K1113	0,92	0,14	

Table 3.
Results of strength tests of the EN AC-AlSi17 alloy

Specimen No.	Ø [mm]	F[kN]	Rm [MPa]	Average [MPa]
1101	15	40	240	
1102	14,9	36,5	206	**214**
1103	15	36	206	
1151	14,8	34	199	
1152	14,9	22,5	124	**149**
1153	15	22,5	125	
1111	14,8	19,5	112	
1112	15	28	159	**128**
1113	14,9	20,05	113	
K1101	14,8	40	240	
K1102	14,8	38,5	230	**228**
K1103	15	37,5	215	
K1151	14,9	25,3	145	
K1152	15	24,2	137	**146**
K1153	14,9	27,2	156	
K1111	15	25,5	145	
K1112	15	22,6	128	**138**
K1113	14,9	24,9	142	

3. Conclusions

Presented work shows impact of vibrations of casting mould in course of crystallization on porosity and mechanical properties of the EN AC-AlSi17 alloy.

Results of investigation of porosity's surface area are illustrated by the following figures:

Table 4.
Results porosity surface area of the EN AC-AlSi17 alloy

Comparison of the specimens	Porosity surface area
115X/110X	Reduction with 10%
111X/110X	Growth with 34%
111X/115X	Growth with 49%
K115X/K110X	Growth with 8%
K111X/K110	Growth with 11%
K1111X/K115X	Growth with 37%
K110X/110X	Reduction with 11%
K115X/110X	Growth with 8%
K111X/110X	Reduction with 33%
K115X/115X	Growth with 20%
K111X/111X	Growth with 10%

- Examining effect of vibrations on size of surface area of porosity we can conclude that vibrations have advantageous effect, because together with growth of vibrations we can notice reduction of size of surface area of porosity [table 2, table 4].
- Making comparison of porosity in specimens poured without vibrations and specimens poured with 0% amplitude of vibrations we can see 10% smaller surface area of porosity.
- If, additionally to vibrations we tilt the metal mould with 20^0 , the reduction amounts to as many as 33%.
- The smallest surface area of porosity was obtained for 0% amplitude of vibrations and tilt angle of 20^0.
- The experiments have confirmed that for the EN AC-AlSi17 alloy the highest growths of tensile strength occur at 0% amplitude of vibrations [table 5].
- Results of the experiments show, that the smallest porosity occurs at 0% amplitude of vibrations tilt angle of 20^0.

Table 5.
Results R_m tensile strength of the EN AC-AlSi17 alloy

Comparison of the specimens	Rm tensile strength
115X/110X	Reduction with 43%
111X/110X	Reduction with 88%
111X/115X	Reduction with 65%
K115X/K110X	Reduction with 56%
K111X/K110X	Growth with 3%
K111X/K115X	Growth with 6%
K110X/110X	Reduction with 4%
K50X/110X	Growth with 6%
K111X/115X	Growth with 55%
K115X/115X	Growth with 2%
K111X/111X	Reduction with 9%

- During crystallization, vibrations have also advantageous effect on mechanical properties.
- Amplitude of vibrations have also effect on R_m tensile strength. At 0% amplitude we can obtain a growth of the strength with about 11% (table 5).
- Tilt of the metal mould does not have so much strong effect on the strength as on porosity.

References

[1] Górny, Z. (1992). *Casting alloys of non-ferrous metals.* WNT, Warszawa (in Polish).

[2] Mondolfo, L. F. (1976). *Aluminium alloys. Structure and Properties.* Butter Wooths, London, Boston.

[3] Pietrowski, S. (1997). Piston silumins. *Krzepnięcie metali i stopów*, Vol. 29, PAN Katowice (in Polish).

[4] Kojima, Y. (2000). Platform Science and Technology for Advanced Magnesium Alloys. *Material Science Forum*, *350-351*, *Trans Tech Publications*, Switzerland, 3-18.

[5] Pietrowski, S. (2001). *Silumins.* Wydawnictwo Politechniki Łódzkiej, Łódź (in Polish).

[6] Wasilewski, P. (1993). Silumins – Modification and its effect on structure and properties, *Krzepnięcie metali i stopów*, Vol. 21, PAN Katowice (in Polish).

[7] Ciućka, T. (2005). Registration of crystallization of AlSi20CuNiAK20 casting alloy with ATND method. *Archives of Foundry Engineering*. 5(17), 45-50.

[8] Ciućka, T. (2006). Crystallization curves of syntetic casting alloy on base of aluminum AlCu7Ni5Fe3. *Archives of Foundry Engineering*. 49-54.

[9] Ciućka, T. (2006). Registration of crystallization of AG51 (AlMg5Si1) casting alloy with ATND method. *Archives of Foundry Engineering*. 6(18), 191-196.

[10] Binczyk, F. & Śleziona, J. (2010). Effect of modyfication on the properties of IN-713C alloy. *Archives of Foundry Engineering*. 9-12.

[11] Krajewski, W.K., Zak, P.L., Orava, J., Greer,A.L. & Krajewski, P.K. (2012). Structural stability of the high-aluminium zinc alloys modified with Ti addition. *Archives of Foundry Engineering*. 61-66.

[12] Medlen, D. & Bolibruchova, D. (2012) The influence of remelting on the properties of AlSi6Cu4 alloy modified by antimony. Archives of Foundry Engineering. 12(1), 81-86. DOI: 10.2478/v10266-012-0016-y.

[13] Walasek**, A. &** Szajnar**,** J. (2012). The mechanism of the surface alloy layer creation for cast steel. *Archives of Foundry Engineering*. 12(1), 115-118. DOI: 10.2478/v10266-012-0022-0.

[14] Ignaszak, Z. (2011). Contribution to determination of the life time of chemically self-hardening mould sand. *Archives of Foundry Engineering*. 11(4), 55-60.

[15] Pezda, J. (2011). Predicting of mechanical properties of EN AB-46000 alloy subjected to dispersion hardening. *Archives of Foundry Engineering*. 11(4), 103-108.

ARCHIVES
of
FOUNDRY ENGINEERING
DOI: 10.2478/afe-2013-0002
Published quarterly as the organ of the Foundry Commission of the Polish Academy of Sciences
ISSN (2299-2944)
Volume 13
Issue 1/2013
9 – 14

Structure and Properties Investigation of MCMgAl12Zn1 Magnesium Alloy

L.A. Dobrzański*, M. Król
Institute of Engineering Materials and Biomaterials, Silesian University of Technology,
Konarskiego 18A, 44-100 Gliwice, Poland
* Corresponding author. E-mail address: leszek.dobrzanski@polsl.pl

Received 02.07.2012; accepted in revised form 04.09.2012

Abstract

This work presents an influence of cooling rate on crystallization process, structure and mechanical properties of MCMgAl12Zn1 cast magnesium alloy. The experiments were performed using the novel Universal Metallurgical Simulator and Analyzer Platform. The apparatus enabled recording the temperature during refrigerate magnesium alloy with three different cooling rates, i.e. 0.6, 1.2 and 2.4°C/s and calculate a first derivative. Based on first derivative results, nucleation temperature, beginning of nucleation of eutectic and solidus temperature were described. It was fund that the formation temperatures of various thermal parameters, mechanical properties (hardness and ultimate compressive strength) and grain size are shifting with an increasing cooling rate.

Keywords: Thermal analysis, Microstructure, Mechanical properties, Magnesium alloy

1. Introduction

Magnesium has the best strength to weight ratio of common structural metals, and it has exceptional die-casting characteristics. This makes magnesium alloys particularly attractive for transportation applications such as in the automotive and aircraft industries for weight reduction and higher fuel efficiency. The rapid growth in the magnesium consumption has highlighted the need for a greater understanding of factors that influence the properties of magnesium alloys and industry's increasing demands for a wider range of magnesium alloys with lower thermal expansion, higher fatigue strength, higher creep strength, and better corrosion resistance [1, 2]. The current use of magnesium in automotive applications is limited to noncritical parts because of its restricted creep properties [3].

The growing interest of many branches of industry magnesium alloys involves the need to carry out research on the optimization of chemical composition and manufacturing technology in order to obtain material which is characterized by the most favourable mechanical properties, and thus the use of modern methods of research of magnesium alloys in real time, in order to achieve full control over the process of crystallization and to make possible the improvement of quality alloy [4, 5].

One of the most common methods for the study of alloys in a liquid state before pouring method of analysis used thermal-derivation. This method is due to its simplicity, has found wide application in assessing the quality of liquid metal alloys. Based on theoretical analysis of phase equilibrium systems, and practical measurements in industrial conditions, can be determined between the temperature dependence of nucleation phase, solidus temperature, cooling rate and chemical composition of the alloy and its properties. A special feature of this method is the short time in which to obtain data to evaluate the test material [6-9].

The derivative thermal analysis is a modernized and extended form commonly known thermal analysis. Registration involves an alloy solidification curve and determining on the basis of the first derivative, which represents the change of state and changes in a liquid state and solid. Thermal derivation analysis can provide valuable derivation of quantitative and qualitative information that are difficult or impossible to obtain by other methods. This allows for better design of alloys, their heat treatment and allows more accurate their assessment.

Thermal derivation analysis is very broad scope in both research and industrial practice. The most common application concerns a field of quality management because it allows rapid assessment of concentrations of certain elements in alloys, evaluation of some mechanical and technological properties, which in turn determines the quality of alloys. Thermal analysis is possible to perform alloy just before casting into the mould to make any adjustments to the quality of molten metal, e.g. for subsequent heating or cooling. The particular advantage this method is not only the opportunity to evaluate alloy with the chemical composition, but also the opportunity to evaluate the same process of measuring many of the details of the kinetics of crystallization of primary or secondary. Obtain as much information on interest in such a short time (2-5 minutes) allows for an immediate decision to improve the quality or the motivates greater technical discipline process. This is so the best and easiest way to improve the quality of foundry and metallurgical deciding the degree of reliability of machines and equipment [10-13].

2. Investigation methodology

Research has been done on MCMgAl12Zn1 magnesium alloys in as-cast made in cooperation with the Faculty of Metallurgy and Materials Engineering of the Technical University of Ostrava and the CKD Motory plant, Hradec Kralove in the Czech Republic. The chemical composition of the investigated material is given in Table 1. A casting cycle of alloys has been carried out in an induction crucible furnace using a protective salt bath Flux 12 equipped with two ceramic filters at the melting temperature of 750±10ºC, suitable for the manufactured material. In order to maintain a metallurgical purity of the melting metal, a refining with a neutral gas with the industrial name of Emgesalem Flux 12 has been carried out. To improve the quality of a metal surface a protective layer Alkon M62 has been applied. The material has been cast in dies with betonite binder because of its excellent sorption properties and shaped into plates of 250x150x25. The cast alloys have been heated in an electrical vacuum furnace Classic 0816 Vak in a protective argon atmosphere.

Table 1.
Average chemical composition (wt. %) of the MCMgAl12Zn1 alloy

Al	Zn	Mn	Cu	Si	Fe
11.894	0.55	0.22	0.0064	0.05	0.02

The thermal analysis during melting and solidification cycles was carried out using the Universal Metallurgical Simulator and Analyzer (UMSA) (Fig. 1) [14]. The melting and solidification experiments for the magnesium alloy were carried out using Argon as cover gas. The data for Thermal Analysis (TA) was collected using a high-speed National Instruments data acquisition system linked to a personal computer. Each TA trial was repeated three times to stabilize a process.

The TA signal was recorded during the melting and solidification cycles. The temperature vs. time and first derivative vs. temperature were calculated.

The procedure comprised of the following steps. First, the test sample was heated to 700±2°C and isothermally kept at this temperature for a period of 90s in order to stabilize the melt conditions. Next, the test sample was solidified at cooling rate of approximately 0,6°C/s, that was equivalent to the solidification process under natural cooling conditions. To achieve an intentional cooling rate:
- 0.6°C/s sample was cooled without forces air
- 1.2°C/s sample was cooled in airflow 30 l/min,
- 2.4°C/s sample was cooled in airflow 125 l/min.

The experiments were performed using a pre-machined cylindrical test sample with a diameter of ϕ=18mm and length of l=20mm taken from the ingot. In order to assure high repeatability and reproducibility of the thermal data, the test sample mass was 9.1g within a very closely controlled range of ±0,1g. Each sample had a predrilled hole to accommodate a supersensitive K type thermocouple (with extra low thermal time constants) positioned at the center of the test sample to collect the thermal data and control the processing temperatures.

Metallographic samples were taken from a location close to the thermocouple tip. Samples were cold mounted and grounded on 240, 320, 400, 600 and 1200 grit SiC paper and then polished with 6μm, 3μm and 1μm diamond paste. The polished surfaces were etched with a solution of 2g oxalic acid, 100ml water, with fresh alcohol blotted repeatedly onto the surface to prevent residue deposits.

Microstructure features were characterized using light optical microscope Leica Q-WinTM image analyzer.

The X-ray qualitative and quantitative microanalysis and the analysis of a surface distribution of cast elements in the examined magnesium cast alloys have been made on the Opton DSM-940 scanning microscope with the TRIDENT XM4 (EDS, WDS, EBSD) EDAX dispersive radiation spectrometer at the accelerating voltage of 20 kV. Phase composition and crystallographic structure were determined by the X-ray diffraction method using the X`Pert device with a copper lamp, with 40 kV voltages. The measurement was performed by angle range of 2θ: 30º-120º.

Rockwell F–scale hardness tests were conducted at room temperature using a Zwick HR hardness testing machine.

Ultimate compressive test were made on universal testing machine Zwick ZHR 100. Compression and hardness specimens were tested corresponding to each of the three cooling rates.

3. Investigation results

According to the X–ray phase analysis, the investigated MCMgAl12Zn1 alloy cooled with solidification rate: 0.6, 1.2 and 2.4. ºC/s is composed of two phases (Fig. 1.): α–Mg solid solution as matrix and $\gamma(Mg_{17}Al_{12})$. In the diffraction pattern of the matrix, the {011} Mg–diffraction line has very intensity. Based on the X–ray phase analysis was found, that changing the cooling rate does not change the phases composition of investigated alloy. The X–ray phase analysis don't ravel occurring of Mg_2Si and phases contains Mn and Al, what suggested that the fraction volume of these phases is below 3%.

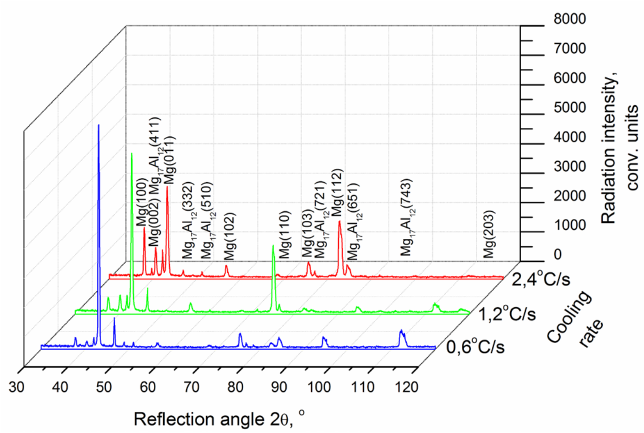

Fig. 1. XRD pattern of MCMgAl12Zn1 casting alloy at various solidification conditions

Figures 2 shows the microstructures of MCMgAl12Zn1 alloys at cooled with different cooling rates. Microstructures consisted of α-Mg solid solution, $Mg_{17}Al_{12}$ phase compound located in grain edge, Mg_2Si and phases contains Mn and Al. The structure configurations at different experimental cooling rates were similar. The cooling rate had obvious effect on grain size of solidification microstructure. The grain size of magnesium alloy was determined by image analysis and shows that the grain size decreases with increasing cooling rate.

SEM micrograph of MCMgAl12Zn1 magnesium alloy after thermal analysis are shown in Fig. 3. Results from EDS analysis are shown in Table 2. EDS spectra for all samples confirms that, the matrix is α-Mg, and intermetallics phases mostly likely Mg_2Si, and Al-Mn (it could be a mixture of Al_8Mn_5, $MnAl_4$). Because the size of particular elements of the structure is, in a prevailing measure, smaller than the diameter of the analyzing beam, the obtained at the quantitative analysis chemical composition may be averaged as a result of which some values of element concentrations may be overestimated.

The cooling curves recorded for MCMgAl12Zn1 alloy at various cooling rates are shown in Fig. 4. Thermal analysis of the magnesium alloys have been presented on Fig. 5. The cooling rate is proportional to the heat extraction from the sample during solidification. Therefore, at a low cooling rate (0.6 ºC/s), the rate of heat extraction from the sample is slow and the slope of the cooling curve is small. So, it creates a wide cooling curve. But, at a high cooling rate (2.4 ºC/s) the rate of heat extraction from the sample is fast, the slope of the cooling curve is steep and it makes a narrow cooling curve. Two visible temperatures were observed on the cooling curves.

More information about the liquidus and solidus temperatures and nucleation of eutectic were characterized based on the first derivative curves (Fig. 5). Thermal analysis of magnesium alloy revealed that the solidify process of material cooled at 0.6°C/s (Fig. 4, line a) started at 583.01± 9.18°C (point 1) and was completed at 420.07±2.97°C (point 3) where fraction solid obtained a 100%.

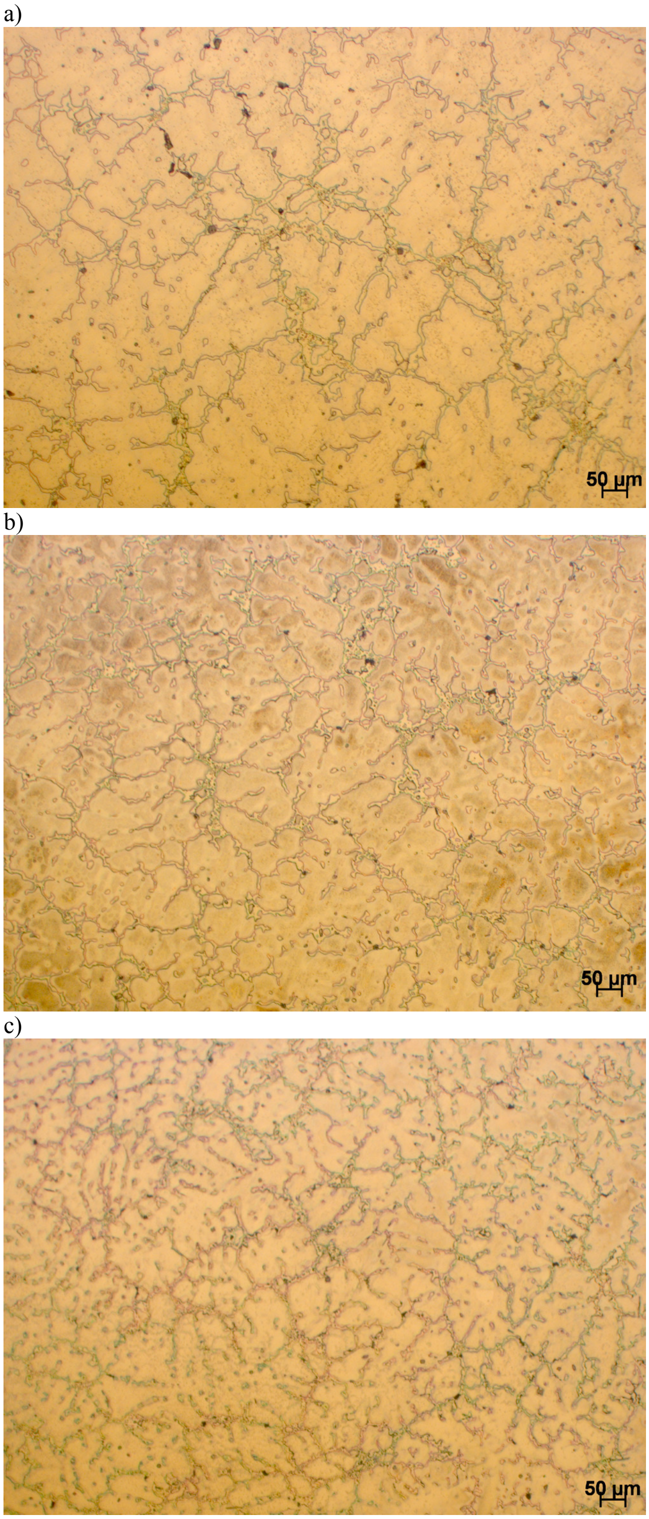

Fig. 2. Microstructures of MCMgAl12Zn1 alloy solidified with cooling rate: a) 0.6°C/s, b) 1.2°C/s, c) 2.4°C/s. Magnification 100x.

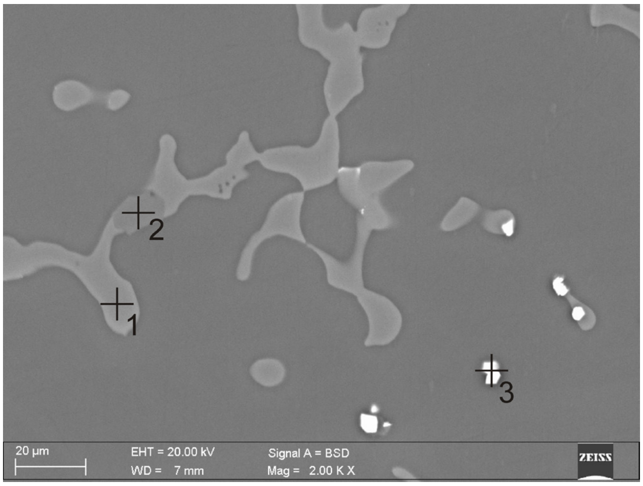

Fig. 3. Representative scanning electron microscope micrograph of magnesium alloy that solidified with cooling rate 0.6°C/s

Table 2.
Pointwise chemical composition analysis from Fig. 3

	Element	*The mass concentration of main elements, %*	
		weight %	*atomic %*
1	Zn	4.17	1.65
	Mg	61.97	65.9
	Al	33.87	32.45
2	Mg	65.86	69.02
	Si	34.14	30.98
3	Mg	8.47	12.47
	Al	41.29	54.79
	Mn	50.24	32.74

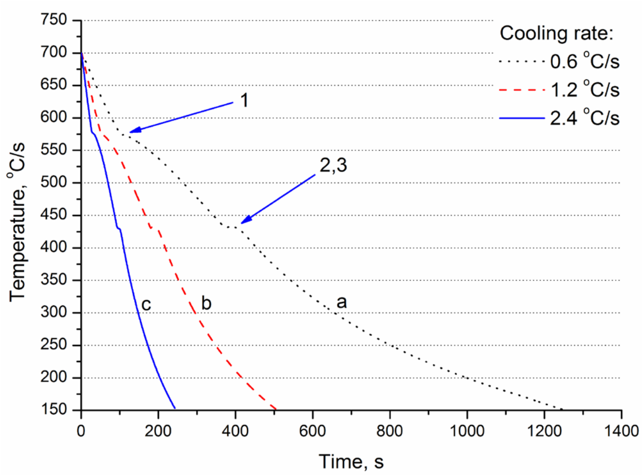

Fig. 4. Temperature vs. time curves of the MCMgAl12Zn1 alloy test samples recorded during solidification at 0.6°C/s (line a), 1.2°C/s (line b) and 2.4°C/s (line c). The numbers correspond to the various metallurgical reactions as presented in Table 3.

Next change on the first derivative curve, at 432.55± 0.64°C was observed and corresponded to the nucleation of the α(Mg)-γ(Mg-$Mg_{17}Al_{12}$) eutectic (Fig. 4, point 2). The cooling curve for the MCMgAl12Zn1 alloy that solidified under a 1.2°C/s solidification rate is presented in (Fig. 4, line b). Alloy started solidify at 582.4±1.98°C and finished at 414.03±3.84°C. The nucleation of the α(Mg)-γ(Mg-$Mg_{17}Al_{12}$) eutectic was observed at 436.05±0.83°C.

The non-equilibrium liquidus temperature of MCMgAl12Zn1 alloy that solidified under a 2.4°C/s (Fig. 4, line c) was found approximately at 592.28±4.64°C. A further decrease in the temperature resulted in nucleation of the α(Mg)-γ(Mg-$Mg_{17}Al_{12}$) eutectic at 441.87±2.24°C. The solidification process finished approximately at 415.42±0.93°C when the fraction solid obtained a 100%.

Table 3.
Non-equilibrium thermal characteristics of the MCMgAl12Zn1 alloy test samples obtained during the solidification process at 0.6°C/s, 1.2°C/s and 2.4°C/s solidification rates

Characteristic point	Solidification rate,°C/s		
	0.6	1.2	2.4
	Temp., °C	Temp., °C	Temp., °C
1	583.01± 9.18	582.4±1.98	592.28±4.64
2	432.55± 0.64	436.05±0.83	441.87±2.24
3	420.07±2.97	414.03±3.84	415.42±0.93

The variations of grain size and ultimate compressive strength have been showed graphically in Fig. 6. Grain size is strictly depending on the cooling rate. For the sample that was cooled with lowest cooling rate, the grain size is approximately 110.4±20 µm. Increases cooling rate cause decrease of grain size to 84.5±8 µm.

Mechanical properties of the magnesium alloy are strongly dependent on the effect of grain size. Ultimate compressive strength increases with a decrease the grain size. Investigations results shows, the increase the cooling rate from 0.6ºC/s to 2.4ºC/s influence on the reduction of the grain size, what have influence on the ultimate compressive strength. The ultimate compressive strength increase from 256.1±9 MPa for lowest cooling rate to 273.7±1 MPa for highest cooling rate (Figure 6).

Figure 7 presents a variation of the hardness as a function of cooling rate. The hardness grows with increment of the cooling rate. The hardness increases from 71.5±1.6 HRF for lowest cooling rate to 74.2±1.8 HRF for highest cooling rate. Measuring errors occurred during testing did not exceed 5%.

a)

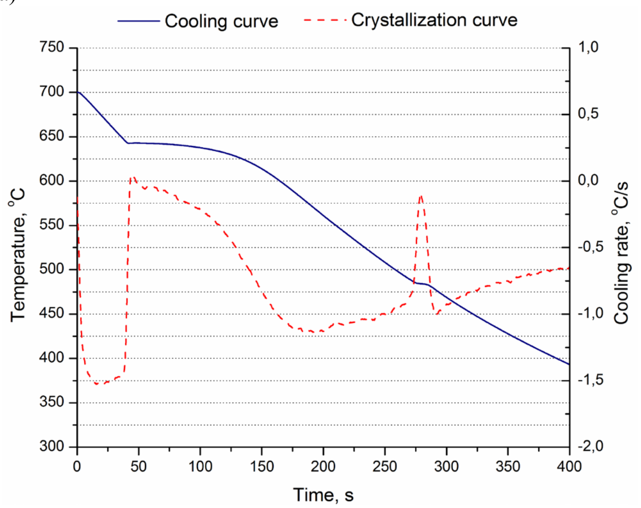

b)

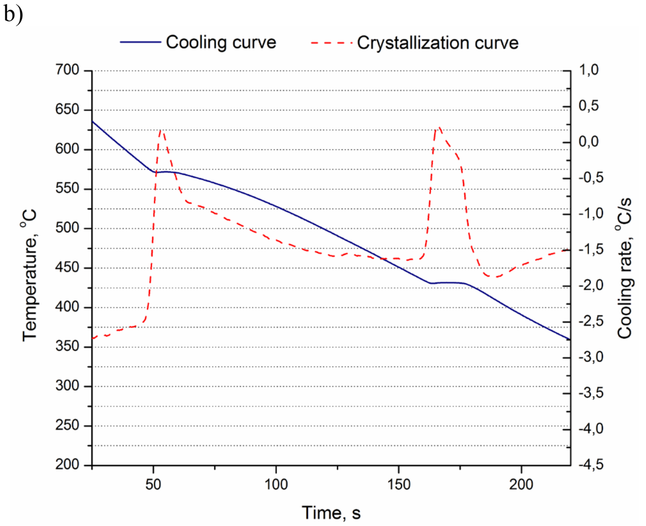

c)

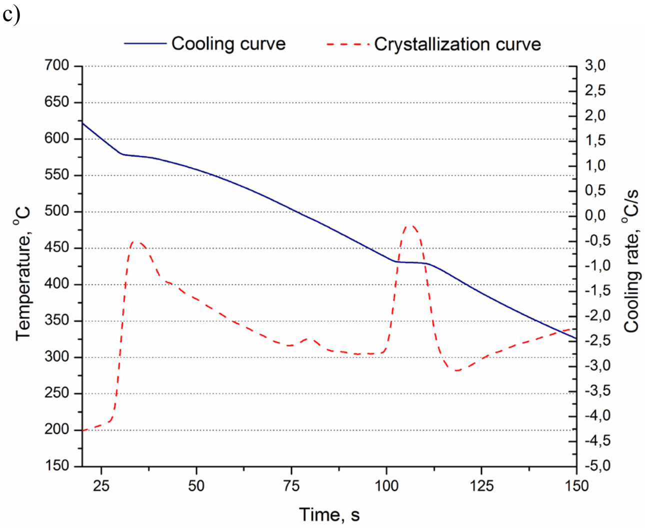

Fig. 5. Cooling and crystallization curves of the magnesium alloy solidified with cooling rate: a) 0.6°C/s, b) 1.2°C/s, c) 2.4°C/s

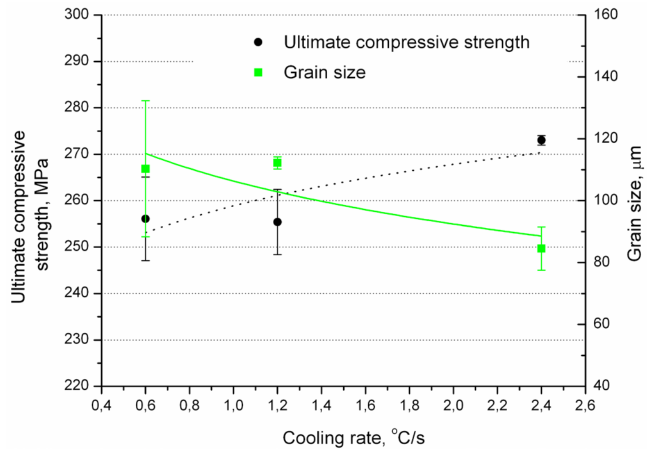

Fig. 6. Variation of the grain size and ultimate compressive strength as a function of cooling rate of analyzed magnesium alloy

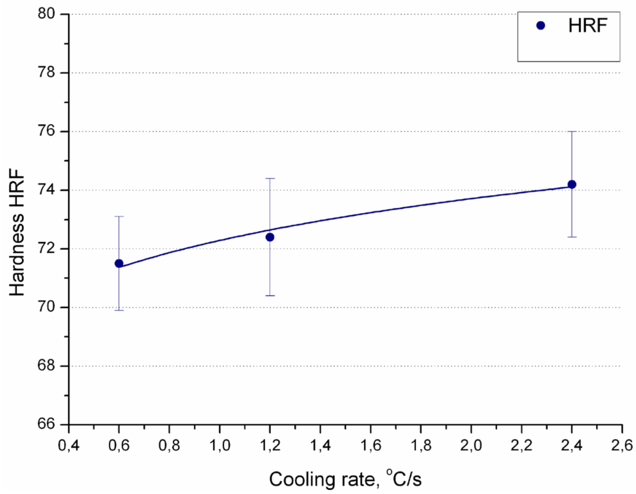

Fig. 7. Variation of the hardness as a function of cooling rate

4. Conclusions

The thermal derivative analysis demonstrates, that diversification of obtained values of phases transformation temperatures, occurring during crystallization and registered on graphs of thermal derivative analysis, are result of changes used cooling rate. Increase of cooling rate causes increase of α phase nucleation temperature and decrease of solidus temperature, causing the increase of temperature range of solidifying alloys.

The α primary solid solution together with the γ-($Mg_{17}Al_{12}$) phase precipitations located mainly in the grains boundaries, α+γ eutectic occurring near $Mg_{17}Al_{12}$ precipitates and Mg_2Si phases ones as well as phases containing Mn and Al make the structure of the examined Mg-Al-Zn cast alloys. The X–ray phase analysis don't ravel occurring of Mg_2Si and phases contains Mn and Al, what suggested that the fraction volume of these phases is below 3%. Change of cooling rate does not result in changes phases compositions of examined alloys. Increase of cooling rate from

0.6°C/s to 2.4°C/s cause decrease of grain size, and thus increase of hardness and ultimate compressive strength.

Acknowledgements

Mariusz Krol is a holder of scholarship from project POKL.04.01.01-00-003/09-00 entitled „Opening and development of engineering and PhD studies in the field of nanotechnology and materials science" (INFONANO), co-founded by the European Union from financial resources of European Social Fund and headed by Prof. L.A. Dobrzanski.

HUMAN CAPITAL NATIONAL COHESION STRATEGY
PROJEKT infonano
EUROPEAN UNION EUROPEAN SOCIAL FUND

References

[1] Guangyin, Y., Manping, L., Wenjiang, D. & Inoue, A. (2003). Mechanical properties and microstructure of Mg-Al-Zn-Si-base alloy. *Materials Transactions.* 44(4), 458-462.

[2] Watanabe, H., Mukai, T., Kamado, S., Kojima, Y. & Higashi, K. (2003). Mechanical properties of Mg-Y-Zn alloy processed by equal-channel-angular extrusion. *Materials Transactions.* 44(4), 463-467.

[3] Mordike, B. L. (2002). Development of highly creep resistant magnesium alloys. *Mater. Sci. Eng.* A324, 103-112.

[4] Djurdjevis, M.B., Kierkus, W.T., Byczynski, G.E., Stockwell, T.J. & Sokolowksi, J.H. (1999). Modeling of fraction solid for 319 aluminum alloy. *AFS Transactions.* 14, 173-179.

[5] Dobrzański, L.A., Maniara, R.& Sokolowski, J.H. (2006). The effect of cast Al-Si-Cu alloy solidification rate on alloy thermal characteristics. *Journal of Achievements in Materials and Manufacturing Engineering.* 17(1-2), 217-220.

[6] Dobrzański, L.A., Kasprzak, W., Kasprzak, M. & Sokolowski, J.H. (2007). A novel approach to the design and optimization of aluminum cast component heat treatment processes using advanced UMSA physical simulations. *Journal of Achievements in Materials and Manufacturing Engineering.* 24(2), 139-142.

[7] Dobrzański, L.A., Maniara, R. & Sokolowski, J.H. (2007). The effect of cooling rate on microstructure and mechanical properties of AC AlSi9Cu alloy. *Archives of Materials Science and Engineering.* 28(2), 105-112.

[8] Dobrzański, L.A., Maniara, R., Sokołowski, J. & Kasprzak, W. (2007). Effect of cooling rate on the solidification behaviour of AC AlSi7Cu2 alloy. *Journal of Materials Processing Technology.* 191, 317-320.

[9] Dobrzański, L.A., Maniara, R., Sokolowski, J.H. & Krupiński, M. (2007). Modelling of mechanical properties of Al-Si-Cu cast alloys using the neural Network, *Journal of Achievements in Materials and Manufacturing.* 20(1-2), 347-350.

[10] Dobrzański, L.A. & Król, M. (2010). Thermal and mechanical characteristics of cast Mg-Al-Zn alloy, *Archives of Foundry Engineering.* 10(1), 27-30.

[11] Dobrzański, L.A., Król, M. & Tański, T. (2010). Influence of cooling rate on crystallization, structure and mechanical properties of MCMgAl6Zn1 alloy. *Archives of Foundry Engineering.* 10(3), 105-110.

[12] Dobrzański, L.A. & Król, M. (2011). Thermal and structure analysis of the MA MgAl6Zn3 magnesium alloy. *Journal of Achievements in Materials and Manufacturing Engineering.* 46(2), 189-195.

[13] Białobrzeski, A. & Pezda, J. (2011). Registration of melting and crystallization process of synthetic MgLi3,5 alloy with use of ATND method. *Archives of Foundry Engineering.* 11(4), 5-8.

[14] Kasprzak, M. (2008). Patent No.: US 7,354,491 B2, United States Patent.

ARCHIVES
of
FOUNDRY ENGINEERING
DOI: 10.2478/afe-2013-0003
Published quarterly as the organ of the Foundry Commission of the Polish Academy of Sciences
ISSN (2299-2944)
Volume 13
Issue 1/2013
15 – 18

Numerical Analysis of Influence of the Mold Material on the Distribution of Shrinkage Cavities

R. Dyja
Institute of Computer and Information Sciences, Czestochowa University of Technology,
ul. J. Dąbrowskiego 73, 42-201 Czestochowa, Poland
Corresponding author. E-mail address: robert.dyja@icis.pcz.pl

Received 05.07.2012; accepted in revised form 04.09.2012

Abstract

Production of castings, like any other field of technology is aimed at providing high-quality product, free from defects. One of the main causes of defects in castings is the phenomenon of shrinkage of the casting. This phenomenon causes the formation of shrinkage cavities and porosity in the casting. The major preventive measure is supplementing a shortage of liquid metal. For supplement to be effective, it is necessary to use risers in proper shapes. Usually, the risers are selected on the basis of determination the place of formation of hot-spots in the castings. Although in these places the shrinkage defects are most likely to occur, shape and size of these defects are also affected by other factors. The article describes the original program setting out the shape and location of possible cavities in the casting. In the program is also taken into account the effect of temperature on the change in volume of liquid metal and the resultant differences in the shape and size of formed shrinkage cavities. The aim of the article is to describe the influence that have material properties of the mold on the simulation results.

Keywords: Application of Information Technology to the Foundry Industry, Castings Defects, Macroshrinkage, Solidification Process, Finite Element Method

1. Introduction

A shrinkage cavity is an open or enclosed area inside the casting, which is not filled with casting material when the solidification ends. Its elimination is impossible. Usually the aim is to ensure that the cavity arose in the places foreseen by the designer of mold. Such a procedure requires that the separate parts of the casting solidify in the correct order, because the solidified as the last are particularly vulnerable to the occurrence of shrinkage cavities. Another solution is using the risers, which act as reservoirs supplying the casting with liquid metal.

The phenomenon of the shrinkage cavities in castings, is mainly due to the difference in density of the liquid and solid phase of material of the casting. Simulations of temperature distribution in the solidifying casting are able to provide some indication about a possible location of the cavities in the casting. However, the location of the cavities is also affected by a number of other factors which should be considered in simulations, such as the existence of channels through which the liquid metal can flow. This topic was also undertaken in the work of other authors [1, 2]. The proposed program takes into account these effects in calculation and presents the results of the simulation in the form of easy to interpret the distributions of the casting area degree of filling.

Although usually the largest change of the casting material density occurs at the transition from the liquid phase into the solid phase, it should be remembered that due to temperature decrease there is also a change in volume of these phases. Change of the liquid phase volume, although it is usually not large and relates to the moment when there is no problem with the flow of liquid metal, may have some impact on the final shape of the shrinkage cavities. This influence on the simulation results is also reflected in presented paper.

2. Description of developed method

2.1. Finite element method

Presented algorithm is based on the results of previous calculations of solidification model. The required results are time depended temperature change and solid phase fraction distribution. Numerical simulations of solidification are based on heat transfer equation with heat source term:

$$\nabla \cdot (\lambda \nabla T) + \dot{q} = c\rho \frac{\partial T}{\partial t} \tag{1}$$

where λ is heat conductivity, T is temperature, c is specific heat, ρ is density, t is time and q is heat source term, which in the case of solidification is related to the phase change phenomena.

Solution of equation (1) is obtained numerically with use of the finite element method [3]. In presented paper time discretization was done with the use of two-step time discretization scheme, represented by Dupont II scheme. The amount of solid phase which grows in solidifying casting was calculated according to intermediate model. The intermediate model assumes full solute diffusion in liquid phase and finite solute diffusion in solid phase. The numerical model uses two types of boundary conditions, namely Newton boundary condition (III type boundary condition) and heat exchange between two regions (IV type boundary condition).

2.2. A determination of the position and size of shrinkage cavities

The author's algorithm used in this paper is an extension of the method presented in [5]. In this method is assumed to have the results of simulation of temperature distribution during the casting solidification obtained using the finite element method. Algorithm also relies on the assumption that the casting area is divided into elements corresponding to triangular finite elements.

The presented algorithm should take into account the behavior of liquid metal consistent with physical laws. Therefore, it is assumed that: the movement of liquid takes place under the effect of gravity, fully solidified canals prevent the motion of liquid, there must be enough liquid metal to compensate for loss caused by the solidification. It is required that every element is described by: solidification time, area, the current amount of liquid metal and a list of adjacent elements. These elements must be sorted ascending according to solidification time. Operation of the proposed method consists of the following steps for each of the elements:

1. Determination the liquid metal loss A_C due to solidification, with the use of formula (2)
2. Finding elements that are not fully solidified and have a connection with the current element.
3. Subtracting amount of the liquid contained in the current element from the A_C.
4. Further subtraction from the A_C amount of the liquid contained in the elements that are connected with the current element [5]. As the first elements are chosen those that have the highest location. Condition of the feeding possibility is that the element that supplies liquid metal has higher location of geometrical center than the current element
5. If there is subtracting the amount of liquid from the A_C occurs updating the degree of filling the current element and element that provides liquid metal. The degree of filling is a ratio of amount of liquid metal in the element and the area of element.
6. The algorithm stops when the value of A_C drops to zero, or when there are no elements that could feed the current element.

The loss of liquid due to solidification is calculated by the following formula:

$$A_C = A_E \cdot (1 + \beta) \tag{2}$$

where A_C is the amount of liquid needed to supply the solidified finite element of given area A_E, and β is a value of volumetric shrinkage.

One of the improvements of this algorithm involves taking into account the volume change of the liquid phase caused by temperature. This requires an earlier determination of the degree of overheating of liquid metal and calculation on this basis the volume change of the liquid phase, which is called in the algorithm 1 liq_loss. Finding the level of the surface of liquid metal is done in accordance with the steps of the algorithm 1. Its input is a list of elements in the casting and the previously mentioned value of the volume change of the liquid phase. The resulting values are arrays containing the amount of liquid metal and the filling ratio of each element, as well as the variable that stores the total amount of liquid metal in the casting.

Algorithm 1 Procedure to determine the level of liquid metal surface taking into account volume changes of the liquid phase
Input: element_list, liq_loss
Output: liq_quant, fill_degree, liq_quant_cast

```
liq_quant_cast = cast_area
1. for each e from element_list:
   1.1. liq_quant[e] = area(e)
   1.2. fill_degree[e] = 1
2. for each e from element_list:
   2.1 if liq_loss – liq_quant[e] > 0 then:
      2.1.1. liq_loss = liq_loss – liq_quant[e]
      2.1.2. liq_quant_cast = liq_quant_cast – liq_quant[e]
      2.1.3. liq_quant[e] = 0, fill_degree[e] = 0
   2.2. else:
      2.2.1.liq_quant[e] = liq_quant[e] – liq_loss
      2.2.2. liq_quant_cast = liq_quant_cast – liq_loss
      2.2.3. fill_degree[e] = liq_quant[e]/area(e)
      2.2.4. liq_loss = 0
3. return liq_quant, fill_degree, liq_quant_cast
```

Moreover, an additional condition was introduced, which assumes preventing the flow of liquid metal through the finite elements that have at least 90% of the solid phase. This condition was introduced to model the resistance of flow of liquid metal caused by the solid phase growth. Taking into account this condition requires a modification of procedure tracing the neighborhood of solidified element. It is necessary to take into account the condition presented in the form of algorithm 2. The input for this algorithm is: an index of the solidified element, an index of the element for which the flow possibility is tested, the list of neighbors of the inspected element and the array that holds the solid phase fraction for all elements at a given moment of time.

Algorithm 2 Procedure to check if an element b makes possible the flow of liquid metal
Input: a, b, neighbor_list, solid_ratio
Output: flow
1. if solid_ratio[b] < 90% then:
    1.1. return flow = true
2. for each e from neighbor_list[e]:
    2.1. if e != a && solid_ratio[e] < solid_ratio[b] then:
        2.1.1. return flow = true
3. return flow = false

The character of this algorithm is based on the fact that the simple introduction of no-flow condition through the elements significantly filled with the solid phase would result in a lack of flow of liquid metal in most of the cast, since the fully solidified elements usually are surrounded by the elements with considerable amount of solid phase. The condition in which it is assumed that the metal can flow in the direction of decreasing the solid phase fraction can overcome this negative phenomenon in the simulation.

3. Description of numerical analysis

The purpose of the analysis was to examine the impact of the mold material on the results obtained from the numerical simulation of the formation of shrinkage cavities.

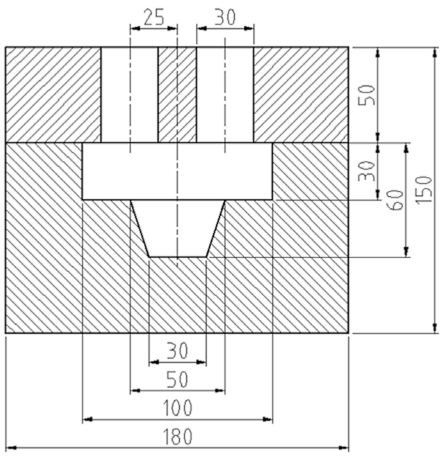

Fig. 1. The shape of the casting used in the simulations

Two variants of the simulation were performed. During the first variant the casting solidifies in the metal mold, while in the second one - in the sand mold. The tests were performed for the shape of the casting shown in Figure. 1.

Numerical simulations of temperature distribution and the solid phase fraction, which are the input to my own program, were carried out in the NuscaS system [6]. This system solves the heat conduction problem using the finite element method. The number of finite elements, which participated in the FEM calculations is equal to 34 529, regardless of the task variant. Simulation of the degree of filling of elements uses the same mesh.

As a material of casting was adopted the alloy of aluminum with addition of 2% copper. This alloy is characterized by a relatively high value of the volumetric shrinkage [9], which value was equal to 6%. Change in the volume of the liquid phase due to temperature decrease was equal to 0.1% for every 10 K, this value was estimated from data for pure aluminum [7]. Other physical properties for this alloy are collected in Table 1.

Table 1.
The physical properties of cast material

Quantity	Unit symbol	Value	
		Liquid phase	Solid phase
Thermal conductivity coefficient	W/mK	104	262
Density	kg/m^3	2498	2824
Specific heat	J/kgK	1275	1077
Solidus temperature	K		877
Liquidus temperature	K		926
Melting temperature of pure metal	K		933
Latent heat of solidification	J/kgK		390000

In Table 2 the physical properties of mold materials used in the simulations are summarized. Data concerning sand mold parameters are taken from [8], and the properties of the metal mold from [4].

The temperature of the liquid metal at the beginning of the simulation was equal to 1150 K. It is assumed that the metal mold was heated to 600 K, while the sand mold had a temperature equal to ambient temperature, ie 300 K.

Table 2.
The physical properties of mold materials

Quantity	Unit symbol	Value	
		Metal mold	Sand mold
Thermal conductivity coefficient	W/mK	24	0.66
Density	kg/m^3	7200	1590
Specific heat	J/kgK	600	1135

For both variants of the calculations the parameters of boundary conditions have the same values. On the upper and side surfaces of the mold the occurrence of Newton boundary condition was assumed, which simulated the heat exchange with the environment, taking into account the heat exchange coefficient of 200 W/m^2K. On the lower surface of the mold, due to difficulty of heat exchange, the value of this coefficient was reduced to 50 W/m^2K. The same value of the heat exchange coefficient was also used for the upper surface of the open risers due to the presumed use of an insulating layer of powder. The value of the ambient temperature was equal 300 K. Heat exchange between casting and mold including boundary condition assumes the heat exchange through the insulation layer of conductivity coefficient of separating layer equal to 1000 W/m^2K.

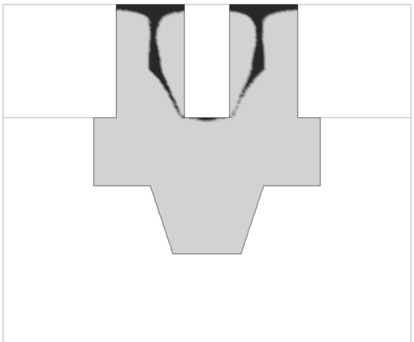

Fig. 2. Cavities in the casting - results for a metal mold

Figure 2 and 3 show the filling of mold at the end of solidification. For the cast solidifying in the metal mold (Fig. 2) shortages in filling of elements appeared only in risers. It suggests that the size of the risers was selected correctly. Due to the fact, that the analyzed shape is symmetric, feeding the cast from both risers follows to the same extent. For this reason in both risers open shrinkage cavities appeared with shape and volume similar to each other.

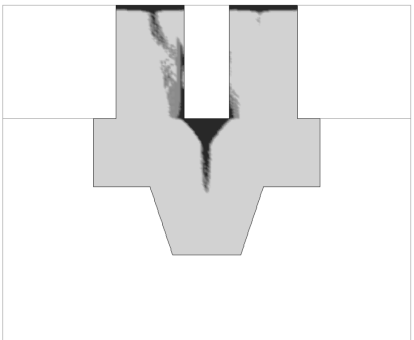

Fig. 3. Cavities in the casting - results for a sand mold

In the case of the sand mold the empty elements appeared in the mere cast. This suggests that for this case the risers in the real casting do not meet their role. This is probably related to the difficult heat dissipation by sand mold. For this reason, despite the use of powder that impede heat exchange between the surface of risers and environment, the casting solidified after its risers and cavities appeared in it.

4. Summary

In this paper the problems associated with determining the location of shrinkage cavities were presented. Simulations of distribution of the filling degree of elements were performed for the two variants of the physical properties of the mold material. These options reflected the case when the casting solidifies in the metal or sand mold. Analyzing the results can be seen a clear influence of conditions of heat dissipation by the casting on the shape and location of shrinkage cavities.

The program now takes into account the change in volume of the liquid phase, which causes a reduction in the level of metal in the risers in obtained results. However, the inclusion of this phenomenon proved to be irrelevant with regard to the possibility of emergence of defects in the casting, because change in the volume of the liquid phase occurs mainly when the casting does not have much solid phase and there are no significant obstacles to the flow of liquid metal.

Simulations also take into account a condition, in which the liquid metal can flow through the element that contains at most 90% of the solid phase. However, in the case of the analyzed shape of the casting, in which there were no narrow canals, it seems to have insignificant effect on the shrinkage cavities distribution.

References

[1] Skrzypczak, T. & Węgrzyn-Skrzypczak, E. (2010). Simulation of shrinkage cavity formation during solidification of binary alloy. *Archives of Foundry Engineering.* 10(1), 147-152.

[2] Sowa, L. (2002). Numerical simulation of the shrinkage cavity within solidifying steel casting. *Archives of Foundry.* 2(4), 245-250 (in Polish).

[3] Zienkiewicz, O.C. & Taylor, R.L. (2000). *The finite element method*. The Basis, Butterworth-Heinemann. Vol. 1, Oxford.

[4] Sczygiol, N. & Szwarc, G. (2000). Approaches to enthalpy approximation in numerical simulation of two-component alloy solidification. *CAMES.* 7, 717-734.

[5] Dyja, R. & Sczygiol, N. (2011). Method for determining the formation of shrinkage defects in the castings. *Archives of Foundry Engineering.* 11(4), 35-40.

[6] Sczygiol, N., Szwarc, G., Olas, T. & Nagórka A. (1997). Object-oriented analysis of solidification modelled by finite elements. *Solidification of Metals and Alloys.* 30, 233-242 (in Polish).

[7] Mutwil, J., Romankiewicz, A. & Romankiewicz R. (2003). Density investigations of liquid aluminium-silicon alloys. *Archives of Foundry.* 3(10), 53-60 (in Polish).

[8] Bokota, A. & Sowa L. (2001). Application of finite element method for modeling of fluidity test. *Archives of Foundry.* 1(1), 52-47 (in Polish).

[9] Stefanescu, D.M. (2009). Science and Engineering of Casting Solidification. Springer Science+Business Media, New York